Journal of South American Earth Sciences 49 (2014) 39–50

Contents lists available at ScienceDirect

Journal of South American Earth Sciences

journal homepage: www.elsevier.com/locate/jsames

U–Pb LA-ICP-MS geochronology of detrital zircon grains from low-grade metasedimentary rocks (Neoproterozoic – Cambrian) of the Mojotoro Range, northwest Argentina

Pamela A. Aparicio González [a,*], Márcio M. Pimentel [b], Natalia Hauser [b], M. Cristina Moya [a]

[a] Universidad Nacional de Salta, Facultad de Ciencias Naturales, Geología, Buenos Aires 177, 4400 Salta, Argentina
[b] Instituto de Geociências, Universidade de Brasilia (UnB), Brazil

ARTICLE INFO

Article history:
Received 22 May 2013
Accepted 5 October 2013

Keywords:
U–Pb
Zircon grains
Low grade metasedimentary rocks
Mojotoro Range

ABSTRACT

The first results of U–Pb detrital zircons were obtained in three lithostratigraphic units of the Puncoviscana Complex in NW Argentina: Chachapoyas, Alto de la Sierra and Guachos Formations. The Chachapoyas Formation has a maximum sedimentation age of 569 Ma and a minimum age of 533 Ma, based on the U–Pb age of an intrusive porphyry granitic. The Alto de la Sierra Formation, composed by sandstones and volcaniclastic rocks, has a maximum age of 543 Ma. A maximum age of 517 Ma is here reported for the deposition of the Guachos Formation, the youngest unit. The contact between the Chachapoyas and Guachos formations is by a tectonic relation, and it's probably coincident with a stratigraphic unconformity between them (unconformity Tilcara I). The Lizoite Formation is overlying by an unconformity (Tilcara II unconformity) the Puncoviscana Complex, and represents the basal unit of the Mesón Group. The provenance zircon data for that formation indicate a maximum depositional age of 513 Ma.

1. Introduction

The Eastern Cordillera basement of the NW of Argentine is a heterogeneous succession of siliciclastic and chemical rocks, intruded by volcanic, subvolcanic and plutonic/subvolcanic rocks, of Neoproterozoic–Early Cambrian age, identified as the "Precambrian basement" (Keidel, 1910) underlying with angular unconformity the Cambrian and Ordovician deposits of the Mesón and Santa Victoria Groups. The unit was defined as the Puncoviscana Formation (Turner, 1960) in the Santa Victoria range (Fig. 1), and was assigned to the Neoproterozoic–Cambrian (Mirré and Aceñolaza, 1972) due to the presence of *Oldhamia*, a fossil trace of the Lower Cambrian. Aceñolaza et al. (1988) and Aceñolaza and Aceñolaza (2005) identify all the basement of the Eastern Cordillera as a heterogeneous group of rocks affected by low-grade metamorphism, the Puncoviscana Formation *s.l.* Zimmermann (2005), correlates this stratigraphic core that outcrops in the Argentinean northwest with the rocks of medium and high metamorphic grade of the eastern Pampean Ranges. This last author identifies the Puncoviscana Formation *s.l.* with the name of *Puncoviscana Complex*, a term according with the nomenclature for metamorphic and sedimentary rocks of the *British Geological Survey* (Hallworth and Knox, 1999). In this paper the Puncoviscana Complex term *sensu article 32* of the Código Argentino de Estratigrafía is used to identify all the stratigraphic core of the Eastern Cordillera.

The lithological heterogeneity of the stratigraphic core of the region was highlighted through different sedimentological and stratigraphical studies, where diverse carbonatic and clastic facies are recognized (Jezek, 1990). These were totally or partially identified in the Sancha, Las Tienditas, Puncoviscana *sensu stricto*, Corralito and Guachos Formations (Salfity et al., 1975; Baldis y Omarini, 1984; Moya, 1998) (Fig. 1).

In the last decade, several studies were carried out in different parts of the Puncoviscana Complex to determine the age of deposition and tectonic setting. Whole rock geochemistry (Omarini et al., 1999; Do Campo and Guevara, 2005; Zimmermann, 2005) and U–Pb studies for different parts of the Eastern Cordillera (Adams et al., 2008; Hauser et al., 2010; Adams, 2011; Escayola et al., 2011) shows a complex population distribution patterns and a heterogeneity in the maximum depositional ages of the Puncoviscana Complex. Many contributions related with the content of ichnofossils of the basement, indicates an Ediacaran-early Cambrian age, currently accepted for the stratigraphic core of the region (Mángano and Buatois, 2004;

* Corresponding author. Tel.: +55 21 34969077.
E-mail addresses: pamelaaparicio@gmail.com (P.A. Aparicio González), marcio@unb.br (M.M. Pimentel), hausernatalia@yahoo.com.ar (N. Hauser), moyacris@arnet.com.ar (M.C. Moya).

0895-9811/$ – see front matter © 2013 Elsevier Ltd. All rights reserved.
http://dx.doi.org/10.1016/j.jsames.2013.10.002

Aceñolaza and Aceñolaza, 2005; Seilacher,2005; Aparicio González et al., 2010; López de Azarevich et al., 2012).

The typical sedimentary characteristics and the original microfabric of the Puncoviscana Complex are well exposed in the Mojotoro Range (Willner, 1990), located to the east of Salta city (Fig. 2). The Puncoviscana complex is unconformably overlayed by the Cambrian Mesón Group (Keidel, 1943) and the Ordovician Santa Victoria Group (Harrington and Leanza, 1975). Recently, Aparicio González et al. (2010), based in sedimentary, mineralogical and geochemical data, recognized three main stratigraphic units in the Puncoviscana Complex at the Mojotoro Range locality: Chachapoyas, Alto de la Sierra and Guachos Formations (Fig. 2). In this paper, U–Pb isotopic data by LA-ICP-MS for detrital zircons from the Chachapoyas, Alto de la Sierra and Guachos formations were used to investigate their provenance patterns and to determine their maximum depositional ages. In addition, we present new U–Pb LA-(HR)-ICP-MS data for the Lizoite Formation that represents the basal unit of the Cambrian Mesón Group (Turner, 1960).

2. Tectonic and geological setting

The central Andean basement records at least two main orogenic events between the break-up of Rodinia at ~750 Ma (Cordani et al., 2003; Meert and Torsvik, 2003; Cawood, 2005), and the Upper Carboniferous amalgamation of Pangea. These are the *Pampean* and *Famatinian Orogenies*.

The *Pampean Orogeny* occurred between 550 and 520 Ma (Aceñolaza and Toselli, 1973) and between 600 and 520 Ma (Ramos, 2008). It was registered in the Eastern Cordillera, Puna and more extensively in the northwestern part of the Eastern Sierras Pampeanas (Aceñolaza et al., 1990; Kraemer et al., 1995; Llambías et al., 1998; Rapela et al., 2001; Vaughan and Pankhurst, 2008). Several hypotheses were proposed by different authors to explain the tectonic evolution of this region during the Late Neoproterozoic–Early Paleozoic i) a passive margin sequence (Ramos, 1988; Jezek, 1990; Sims et al., 1998; Adams et al., 2008, 2011; Schwartz et al, 2008) ii) an intracontinental rift that evolved to an active plate margin (Omarini et al., 1999; Ramos, 2008 iii) a foreland basin (Kraemer et al., 1995; Keppie and Bahlburg, 1999; latter Zimmermann, 2005; Escayola et al., 2011) iv) fore-arc setting (Rapela et al., 2007; Hauser et al., 2010; Escayola et al., 2011) and v) Lucassen et al. (2000) postulate (based in petrological, geochemical and isotopic features of high-grade rock units of the Argentinean and Chilean basement between latitudes 21° and 26° S) the existence of one wide long-lived mobile belt during the evolution of this part of the Central Andes, during in the Early Paleozoic.

The Pampean basement in NW Argentina is intruded by Early Cambrian igneous rocks, whose ages are coeval with the Pampean Cycle. The intrusive granitoid rocks recognized in the Eastern Cordillera basement are also related to this cycle. To the west of the Eastern Cordillera these rocks are known as the Tastil batholith and the Nevado de Chañi granite. The Tastil batholith includes three Cambrian magmatic phases: 1) gray granodiorite, U–Pb age of 535 Ma; 2)

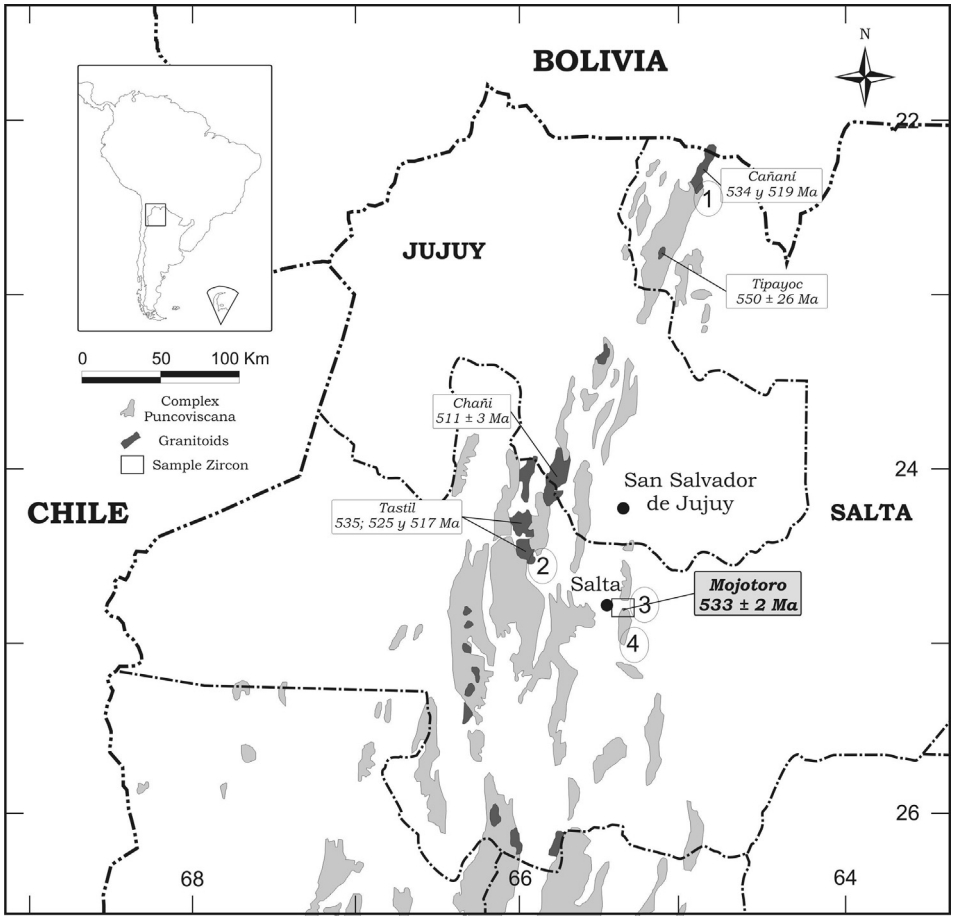

Fig. 1. Simplified map of the main outcrops of the Upper Neoproterozoic Lower Paleozoic basement in central and northern Argentina showing the location of: 1, Santa Victoria Range; 2, Mojotoro Rage; 3, Tastil area; 4, Castillejo Range (Aparicio González et al., 2011).

porphyritic dacite, 525 Ma U–Pb age and 3) red granite, U–Pb age of 517 Ma; and 3) porphyritic dacite, 525 Ma U–Pb age (Bachmann et al., 1987; Hongn et al., 2010; Hauser et al., 2010). Zapettini et al. (2008) reported a zircon U–Pb age of 511 ± 3 Ma (Fig. 1) on the Chañi granite.

Hauser et al. (2010), based on maximum and minimum U–Pb ages for the sedimentary and intrusive igneous rocks in the Tastil area (Fig. 1), shows that the depositional age of the Puncoviscana Complex ranges between 560 and 534 Ma. Also based on U–Pb and Lu–Hf combined data, these authors interpreted the existence of two main magmatic arcs during the Pampean Cycle 1) a pre-Tilcarian arc with zircon population peak at 560 Ma (Late Brasiliano/Early Pampean arc) and 2) a Post-Tilcarian arc with zircons population peak at 530 Ma (Pampean Arc).

Escayola et al. (2011) have recently recognized a felsic tuff layer, interbedded with the sedimentary rocks, close to the Puncoviscana type locality, and reported an U–Pb age of 537 ± 0.9 Ma.

2.1. Local geology: the basement of the Mojotoro Range

The Mojotoro Range, generally an anticline with an axial plane of N–S trend, is located in the southeastern section of the Eastern Cordillera in the NW of Argentine. The core of the anticline structure is composed by a low grade metamorphic complex identified as the Puncoviscana Complex. Recently, the Puncoviscana Complex in the Mojotoro area, was divided into three main units: Guachos, Alto de la Sierra and Chachapoyas Formations (Moya, 1998; Aparicio González et al., 2010) (Fig. 2).

The succession is unconformably overlayed by the Lizoite, Campanario and Chahualmayoc Formations of the Mesón (Keidel, 1943) and (Santa Rosita y Acoite Formations) Santa Victoria Groups (Harrington and Leanza, 1975), with Cambrian and Ordovician ages respectively. In the southern and eastern part of the structure (Fig. 2), are recognized outcrops of the sedimentary succession of the Salta and Oran Groups, with Cretaceous-Eocene and Neogene ages.

The Puncoviscana Complex in the Mojotoro Range is a lithologically and structurally heterogeneous complex. Such complexity is identified by the presence of two sets of rocks showing different structural styles. These different styles are recognized mainly in the folding and structural trends indicating the existence of a tectonic discontinuity (fault) or a sedimentary unconformity (Hongn, 1996).

Moya (1998, 2008) describe two groups of rocks of the basement, showing different degrees of deformation: one of Neoproterozoic age identified as the Sancha Formation (Salfity et al., 1975) located to the west of the Mojotoro range (Fig. 1), and another one of a possible Cambrian age forming the Guachos Formation.

However, the Sancha Formation was originally defined in the Castillejo Range (Fig. 1), in association with the limestones of Las Tienditas Formation. The few geological information about Sancha Formation allows to define that it's a different lithostratigraphic unit, named as the Chachapoyas Formation (Aparicio Gonzalez

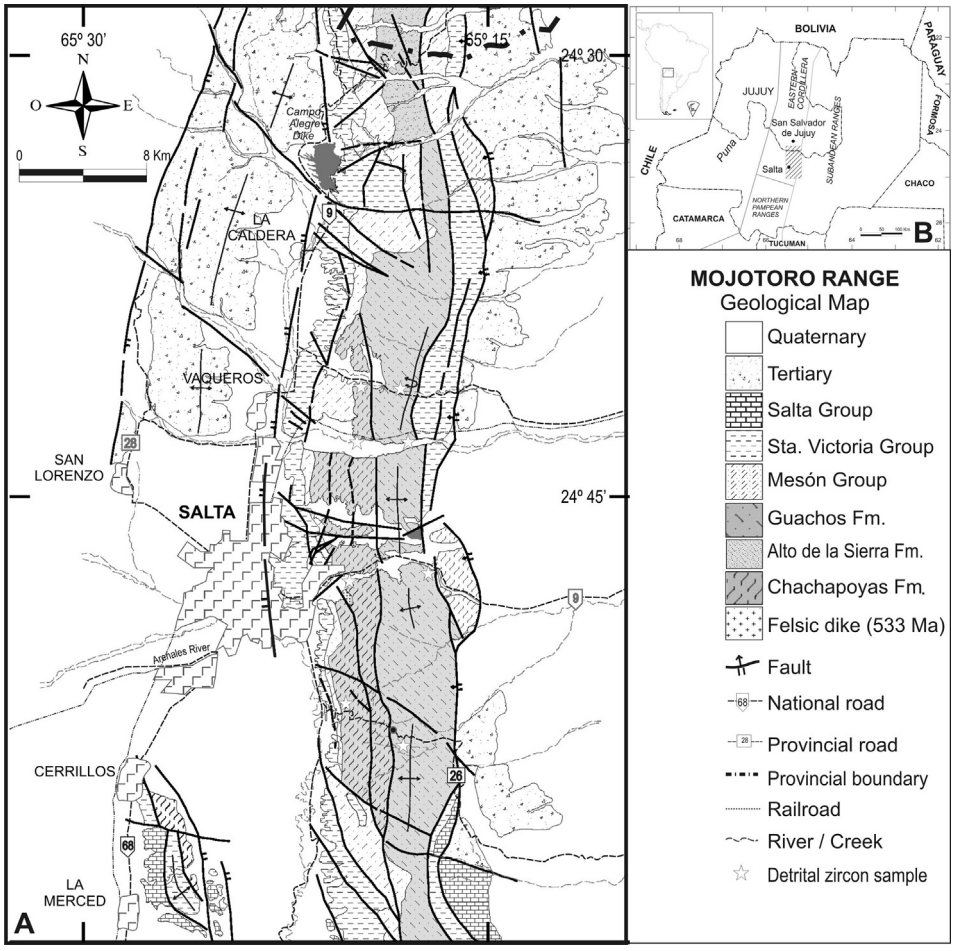

Fig. 2. A: Geological map of the Mojotoro Range showing the subdivision of the different stratigraphic units (modified from Amengual et al., 1979; Moya, 1998). B: Geological map of northwestern of Argentina, showing the different geological provinces.

et al., 2010). This hypothesis is based on field and laboratory detailed study that is presented in this paper.

2.2. Studied units

The **Chachapoyas Formation** (Aparicio González et al., 2010) is exposed along the western flank of the Mojotoro range (Fig. 2). Towards to the west, the sequence unconformably underlies the Lizoite Fm. (Tilcara unconformity) and towards to the east it's in a tectonic contact with the Guachos Formation (Fig. 2). In the central part of the Mojotoro Range, the unit is intruded by felsic dykes, dated U–Pb LA-ICP-MS at 533 ± 2 Ma (Aparicio González et al., 2011). It composed by shales and very fine grained greenish sandstones, displaying a cleavage parallel to the axial plane of the folds. Clay mineralogy corresponds to illite and chlorite. The rocks are strongly folded and affected by an anquizone – epizone metamorphic grade (Fig. 3a).

The **Alto de la Sierra Formation** (Aparicio González et al., 2010) is characterized by layers of purple and gray sandstones, exposed in the northern part of the Mojotoro Range. In the western flank of the structure, the sequence is unconformably overlayed by the Mesón Group (unconformity Tilcara II), and in the eastern part of the structure, it's in tectonic contact with the Lizoite Formation (Fig. 3c). In the western flank of the anticline, the unit is composed by shales and greywackes. Volcaniclastic material is recognized in thin sections, and clay mineralogy corresponds to illite and interlayered illite/smectite. The unit was affected by very low grade metamorphism (Fig. 3d).

The **Guachos Formation** (Moya, 1998) crops out in the central part of the Mojotoro Range and is characterized by a rhythmic sequence of sandstones and shales, mainly with a NE–SW structural trend. The contacts between this unit with the Ordovician rocks of the Santa Victoria Group towards to the east, and with the Chachapoyas Formation towards to the west, are tectonic. The sequence is heterolithic and composed by brown to greenish brown shaly sandstones, characterized by the presence of *Nereites* ichnofacies. The sandstones are mainly composed by quartz, and a minor proportion of felsic volcaniclastic grains.

Fig. 3. A-Fine-grained, greenish, sandstones, underlying the Mesón Group in the Mojotoro river section (Chachapoyas Formation) B-Interbedded sandstone and mudstone deposits in the Guachos Formation. C-Tilcaric II angular unconformity between the Alto de la Sierra Formation and the Mesón Group. D-Photomicrograph of the Alto de la Sierra Formation metawacke (crossed nicols), showing polycrystalline and monocrystalline quartz (Qm), volcanic lithic fragments (Lv), feldspars (potassium FK and plagioclase P) and sedimentary lithic fragment (Ls).

Shales are made of illite, illite/chlorite and chlorite. The Kubler index measured in the pelitic facies of this sequence indicates that was affected by a metamorphism in the high anquizone–epizone field (Fig. 3b).

The **Lizoite Formation** (Turner, 1960) crops out in the central-western part of the Mojotoro Range. The sequence overlies, in angular unconformity, the Chachapoyas and Alto de la Sierra formations, while the contact with the Guachos Formation is by tectonic. The Lizoite Formation is made up of a basal pink conglomerate followed by white/pink quartzites. The conglomerate include rounded and subrounded clasts of quartzite and milky-white quartz in a purple brown sandy matrix, whereas the quartzite succession is composed by quartzite and white to light pink fine-grained quartz sandstones forming 30–60 cm thick layers.

3. Analytical methods

Four sandstone samples from the Alto de la Sierra, Chachapoyas, Guachos and Lizoite Formations were selected for this study. Zircon grains were separated from 1 kg rock samples, one from each section, using standard crushing and heavy mineral concentration techniques at the Universidad Nacional de Salta, Argentina. Magnetic separation using a Frantz isodynamic separator was carried out at the Geochronology Laboratory of the University of Brasilia, only to eliminate strongly magnetic

Table 1
Zircon U–Pb data for metasedimentary rocks of Chachapoyas Formation, Mojotoro range-NW Argentina.

Sample	Ratio						Rho	Ages						% Disc
	$^{207}Pb/^{206}Pb$	1σ (%)	$^{207}Pb/^{235}U$	1σ (%)	$^{206}Pb/^{238}U$	1σ (%)		$^{207}Pb/^{206}Pb$	1σ (Ma)	$^{207}Pb/^{235}U$	1σ (Ma)	$^{206}Pb/^{238}U$	1σ (Ma)	
Chachapoyas Formation-sample RM1														
Z9	0.05835	0.9	0.6950	1.5	0.08638	1.2	0.82	542.9	18.7	535.8	6.2	534.1	6.3	100
Z36	0.05694	1.3	0.6836	2.0	0.08706	1.6	0.77	489.4	28.5	528.9	8.4	538.1	8.1	102
Z40	0.05811	1.0	0.7088	1.3	0.08847	0.8	0.64	533.9	21.5	544.1	5.4	546.5	4.3	100
Z11	0.05854	1.4	0.7331	1.8	0.09083	1.1	0.64	549.9	29.8	558.4	7.7	560.4	6.1	100
Z22	0.05937	0.8	0.7449	4.1	0.09099	4.0	0.98	580.7	18.3	565.2	17.6	561.4	21.5	99
Z50	0.05818	1.5	0.7304	1.8	0.09105	1.1	0.59	536.7	31.7	556.8	7.7	561.7	5.7	101
Z27	0.05958	2.0	0.7599	2.4	0.09250	1.3	0.54	588.2	43.0	573.9	10.4	570.3	7.1	99
Z55	0.05801	1.0	0.7421	1.8	0.09277	1.5	0.84	530.2	21.7	563.6	7.8	571.9	8.3	101
Z7	0.05813	1.6	0.7586	1.9	0.09465	1.1	0.55	534.8	34.9	573.2	8.4	583.0	6.0	102
Z21	0.06042	0.9	0.7911	4.7	0.09497	4.6	0.98	618.6	20.3	591.8	20.7	584.9	25.4	99
Z39	0.06000	1.2	0.8507	1.4	0.10283	0.8	0.56	603.6	25.4	625.0	6.6	631.0	4.8	101
Z5	0.05961	0.8	0.8533	1.5	0.10382	1.3	0.86	589.3	17.1	626.5	7.1	636.8	7.9	102
Z60	0.05995	0.8	0.8713	1.9	0.10541	1.7	0.91	601.8	17.3	636.3	9.0	646.0	10.7	102
Z8	0.06083	0.8	0.9329	1.4	0.11122	1.2	0.83	633.2	16.5	669.1	6.8	679.9	7.4	102
Z28	0.06341	0.8	0.9954	1.3	0.11385	1.1	0.80	722.1	17.0	701.5	6.8	695.1	7.1	99
Z24	0.06236	1.0	0.9812	1.4	0.11412	1.0	0.71	686.4	20.7	694.2	7.0	696.7	6.5	100
Z49	0.06151	0.9	0.9708	1.5	0.11447	1.2	0.81	657.0	18.1	688.9	7.2	698.7	7.8	101
Z42	0.06580	0.9	1.1987	1.6	0.13213	1.3	0.82	800.0	19.5	800.0	9.0	800.0	10.1	100
Z18	0.06654	0.7	1.2430	4.1	0.13549	4.1	0.99	823.4	14.5	820.2	23.0	819.1	31.2	100
Z25	0.07020	1.0	1.4510	1.4	0.14990	1.1	0.73	934.2	19.8	910.3	8.6	900.4	8.8	99
Z47	0.07080	1.6	1.5752	2.5	0.16136	1.9	0.77	951.7	32.7	960.5	15.5	964.3	17.2	100
Z3	0.07181	0.7	1.5122	1.4	0.15273	1.3	0.87	980.5	14.5	935.3	8.8	916.2	10.7	98
Z38	0.07214	0.7	1.7197	1.1	0.17288	0.9	0.80	990.0	13.9	1015.9	7.3	1028.0	8.6	101
Z29	0.07251	0.8	1.7081	1.3	0.17085	1.0	0.80	1000.4	15.8	1011.6	8.2	1016.8	9.7	101
Z37	0.07255	0.7	1.7193	1.4	0.17187	1.2	0.86	1001.4	14.4	1015.7	9.0	1022.4	11.4	101
Z23	0.07295	0.8	1.6991	3.7	0.16893	3.6	0.98	1012.6	16.3	1008.2	23.1	1006.2	33.1	100
Z16	0.07347	1.1	1.8545	2.2	0.18306	1.9	0.86	1026.9	22.4	1065.0	14.4	1083.7	18.9	102
Z57	0.07383	1.0	1.7537	1.7	0.17227	1.4	0.82	1036.9	20.0	1028.5	11.2	1024.6	13.5	100
Z17	0.07392	0.9	1.8619	4.7	0.18269	4.6	0.98	1039.2	18.6	1067.7	30.6	1081.7	45.8	101
Z26	0.07400	0.8	1.8269	1.4	0.17905	1.1	0.79	1041.5	16.6	1055.2	8.9	1061.8	10.6	101
Z48	0.07401	0.9	1.8842	1.7	0.18465	1.4	0.82	1041.6	18.9	1075.5	11.0	1092.3	13.8	102
Z52	0.07432	0.7	1.9237	1.3	0.18773	1.1	0.85	1050.1	14.0	1089.3	8.7	1109.1	11.3	102
Z58	0.07434	1.1	1.8644	1.9	0.18189	1.6	0.83	1050.8	21.5	1068.6	12.5	1077.3	15.6	101
Z15	0.07439	0.9	1.7189	1.5	0.16759	1.2	0.81	1052.0	17.4	1015.6	9.4	998.8	10.9	98
Z19	0.07518	0.6	1.8692	3.7	0.18033	3.6	0.98	1073.2	12.6	1070.2	23.9	1068.8	35.4	100
Z59	0.07573	0.8	2.0142	1.5	0.19292	1.3	0.87	1087.8	15.1	1120.3	10.4	1137.2	13.9	102
Z44	0.07573	0.6	1.9935	1.3	0.19092	1.1	0.88	1088.0	12.1	1113.3	8.5	1126.3	11.4	101
Z41	0.08102	0.7	2.1492	1.8	0.19238	1.7	0.93	1222.0	12.9	1164.8	12.4	1134.3	17.5	97
Z1	0.08205	0.7	2.3480	1.3	0.20755	1.1	0.84	1246.7	13.3	1227.0	9.0	1215.8	11.8	99
Z12	0.09712	0.8	3.7783	1.4	0.28215	1.1	0.81	1569.6	15.2	1588.1	11.2	1602.2	16.1	101
Z46	0.11046	0.6	5.3547	1.6	0.35158	1.4	0.92	1807.0	11.0	1877.6	13.2	1942.1	23.9	103
Z33	0.11389	0.6	5.0992	1.6	0.32473	1.4	0.91	1862.3	11.5	1836.0	13.1	1812.8	22.4	99
Z6	0.11946	0.6	6.0152	1.1	0.36520	0.9	0.81	1948.1	11.4	1978.0	9.3	2006.8	14.9	101
Z14	0.11963	0.8	5.9819	2.3	0.36266	2.2	0.94	1950.7	13.9	1973.2	20.2	1994.8	37.8	101
Z45	0.12009	0.6	6.1163	1.5	0.36940	1.4	0.93	1957.5	10.0	1992.6	13.2	2026.6	24.5	102
Z35	0.12777	1.2	6.5214	1.7	0.37018	1.1	0.66	2067.5	21.8	2048.8	14.6	2030.2	19.3	99
Z2	0.13326	0.7	6.9817	1.3	0.37998	1.1	0.85	2141.4	11.8	2109.1	11.5	2076.2	19.7	98
Z30	0.16654	0.6	11.6869	1.6	0.50897	1.4	0.92	2523.1	10.5	2579.6	14.5	2652.2	31.1	103
Z13	0.17486	0.6	12.7122	1.6	0.52727	1.5	0.92	2604.7	10.5	2658.6	15.4	2729.9	33.8	103
Z4	0.17618	0.7	12.3857	1.3	0.50987	1.1	0.84	2617.2	11.8	2634.1	12.1	2656.1	23.6	101
Z34	0.17644	0.5	11.9724	1.3	0.49214	1.2	0.91	2619.7	9.0	2602.2	11.9	2579.9	24.6	99
Z53	0.17668	0.6	12.6688	1.5	0.52004	1.4	0.91	2622.0	10.5	2655.3	14.2	2699.3	30.4	102
Z10	0.18769	0.7	13.4418	1.4	0.51940	1.3	0.86	2722.1	12.0	2711.2	13.6	2696.7	27.5	99

mineral phases. Randomly picked zircon grains were mounted in epoxy slabs, then polished to obtain a smooth surface, and cleaned in nitric acid prior to analysis. Backscatter electrons (BSE) images were used for spot targeting. BSE images were acquired with a JEOL JXA-8230 scanning electron microscope at the Instituto de Geociências of the Brasilia University, Brasila, Brazil. Once fully dry, the samples were mounted in a specially adapted laser cell for thick sections, and loaded into UP 213 Nd:YAG laser ($\chi = 213$ mm), linked to a Neptune ICPMS. Helium was used as the carrier gas and mixed with Argon before entering the ICPMS.

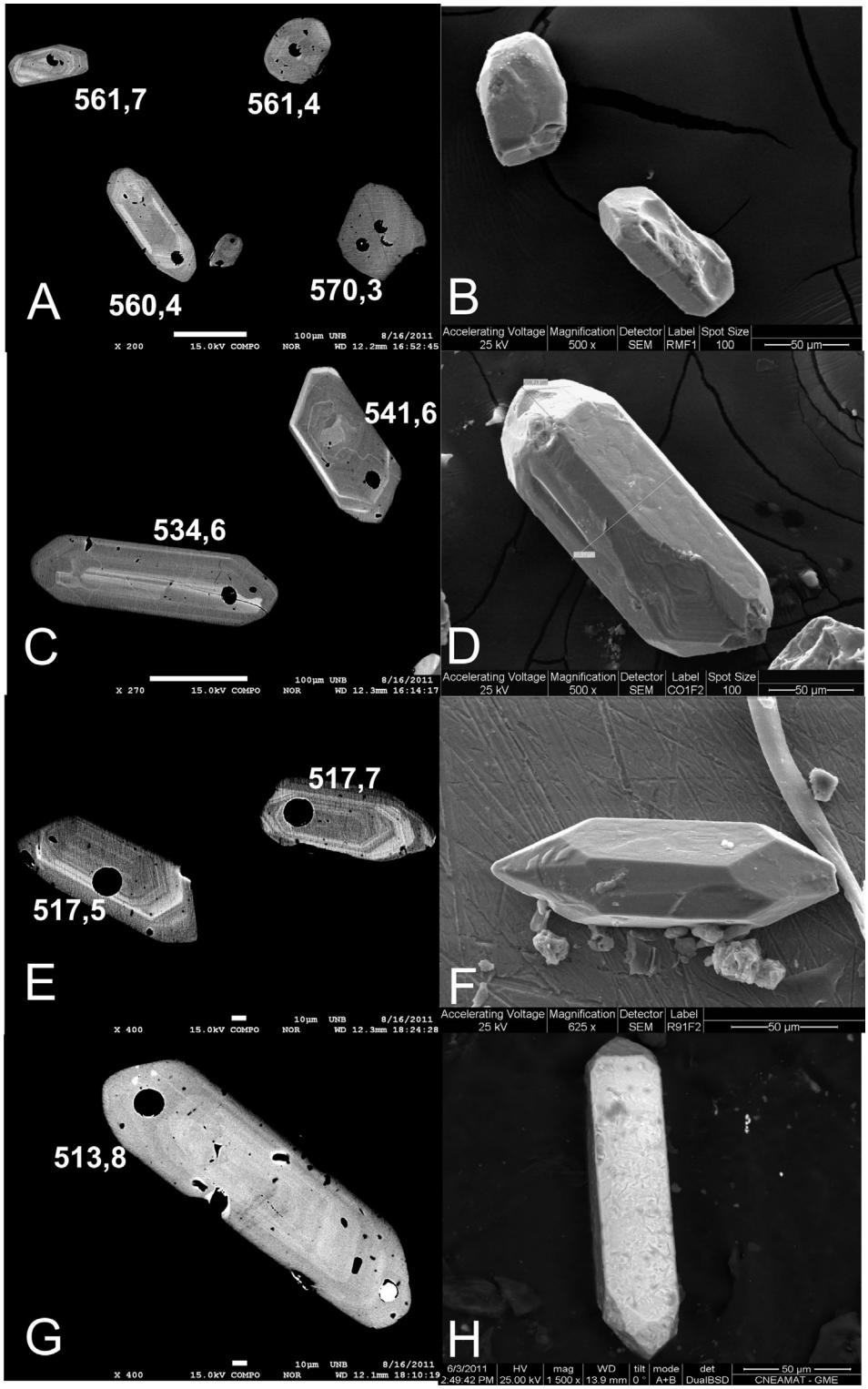

Fig. 4. Back-scattering images and Scanning electron microscope images of representative analyzed zircons. Igneous zircons from (a, b) sample RM1-Chachapoyas Formation (c, d) sample CO1, from the Alto de la Sierra Formation (e, f) sample R 91, from the Guachos Formation (g, h) sample L1, from the Lizoite Formation.

All analyses were conducted in static mode with a laser beam diameter of 30 μm, operated with an output energy of 34% and a pulse rate of 10 Hz. Normalization was carried out using GJ1 standard zircon (608.5 ± 1.5 Ma) (Jackson et al., 2004) and age calculation were performed using an in-house developed Excel worksheet, based on ISOPLOT V3 formulas (Ludwig, 2003). Corrections for common Pb were applied to samples with $^{206}Pb/^{204}Pb$ lower than 1000, using Stacey and Kramers (1975) model at the age of crystallization. U–Pb data were plotted using ISOPLOT V3 (Ludwig, 2003). Errors for isotopic ratios are presented at 1σ level.

4. Results: U–Pb ages

Fifty three U–Pb analyses on single grains, for the **Chachapoyas Formation** (sample RM1), were carried out (Table 1). The zircon grains are up to 150 μm in length, prismatic to sub-rounded (Fig. 4a,b). The data form a polimodal zircon distribution, with a main population with Neoproterozoic–Mesoproterozoic ages, from 800 to 1088 Ma (38% of grains) and a second important population with Cambrian-Neoproterozoic ages, from 534 to 699 Ma (32% of grains). Minor populations with Mesoproterozoic (6%), Paleoproterozoic (13%) and Neoarchean (11%) ages are also observed. In the main population a main peak at 1046 Ma and minor peaks at 803 and 1224 Ma may be recognized, whereas in the second most abundant population several peaks at 562, 694, 547 and 631 Ma, are identified. The Mesoproterozoic, Paleoproterozoic and Neoarchean minor groups, show peaks at 1224, 1955 and 2620 Ma, respectively (Fig. 5a,e,i).

Thirty seven U–Pb analyses on single grains, for the **Alto de la Sierra Formation** (sample CO1), were carried out (Table 2). The zircon grains are up to 200 μm in length, prismatic to sub-rounded, with magmatic zonation (Fig 4c,d). The data form a unimodal distribution, with a main population crystallized between 527 and 798 Ma (62% of grains) and a second population crystallized between 1053 and 1527 Ma (16% of grains). In the main population, two main Neoproterozoic peaks, at 547 and 558 Ma are identified. Zircon with Paleoproterozoic ages (22% of grains) are also observed (Fig. 5b,f,j).

Forty-six U–Pb analyses on single grains, from the **Guachos Formation** (sample R91), were carried out (Table 3). The zircon grains are, up to 150 μm in length, prismatic to sub-rounded, with some grains showing magmatic zonation (Fig. 4e,f). The data form a polimodal zircon distribution, with a main population crystallized between 517 and 810 Ma (50% of grains), a second population crystallized between 926 and 1283 Ma (35% of grains) and minor populations with Paleoproterozoic (11%) and Neoarchean (5% of grains) ages. In the main group, three peaks at 517, 554 and 650 Ma are observed, and in the second population, peaks at 1004 and 1051 Ma were identified (Fig 5c,g,k).

Forty-nine U–Pb analyses on single grains for the **Lizoite Formation** (sample L1), were carried out (Table 4). The zircon grains are large to medium, up to 200 μm in length, prismatic to sub-rounded, with magmatic zonation (Fig. 4g,h). The data form a unimodal zircon distribution, with a main population crystallized between 502 and 598 Ma (86% of grains) with two main peaks at 532 and 556 Ma. A small Mesoproterozoic/Neoproterozoic zircon

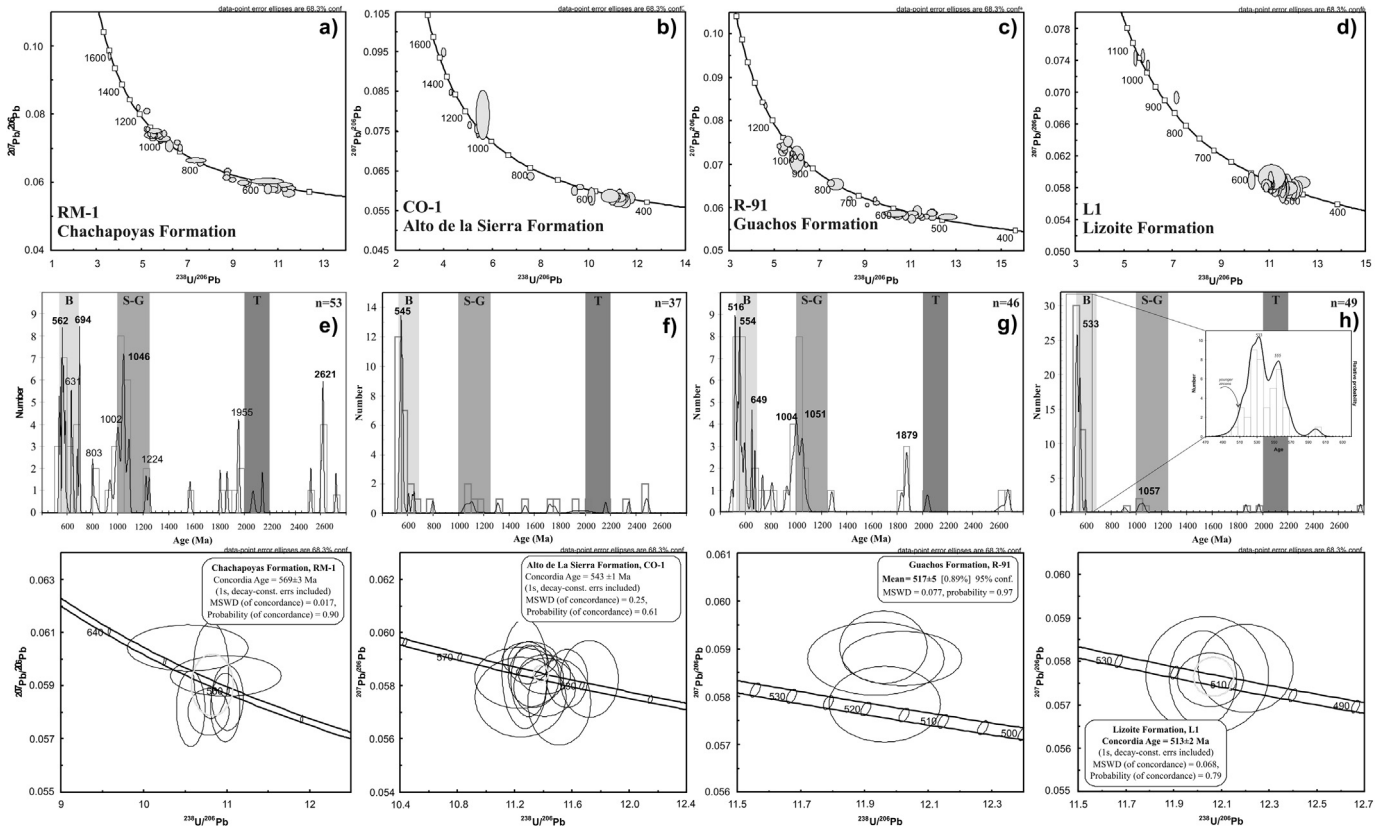

Fig. 5. U–Pb detrital zircon results for Puncoviscana Complex in the Mojotoro Range. Tera-Wasserburg Concordian, (figures a–d with ages between 1600 and 400 Ma) and probability density plot diagrams (figures e–g, with ages between 2800 and 400 Ma) for Chachapoyas, Alto de la Sierra, Guachos and Lizoite Formations, are shown. In the probability density plot diagram the $^{207}Pb/^{206}Pb$ and the $^{238}U/^{206}Pb$ ages have been used for zircons older and younger than 900 Ma, respectively. The vertical gray bands shown in the figure represent the conventional age ranges of Brasiliano–Pampean (B: 530–680 Ma), Sunsas–Grenvillian (S–G: 1000–1250 Ma) and Transamazonian (T: 2.0–2.2 Ga) crustal sources.

population with ages between 906 and 1062 Ma (8% of grains) is recognized. Four Paleoproterozoic zircons (4% of the grains) and one Neoarchean zircon (2% of grains) are also observed (Fig 5d,h,l).

5. Discussion: provenance and age of the Puncoviscana Complex in the Mojotoro Range

The new U–Pb detrital zircon data obtained on four units of the Mojotoro range provide new constraints about the evolution of the western margin of Gondwana.

The sandstone sample (RM-1), of Chachapoyas Formation, shows and heterogeneous zircon distribution. The main population (38%) is dominated by zircons with ages between 800 and 1088 Ma, that indicates a main provenance from the Sunsas–Grenvillian orogen (Cordani et al., 2000; Schwartz and Gromet, 2004), exposed at the southwestern margin of the Amazonian Craton. The second population (32%) shows ages between 534 and 699 Ma, with main peaks at 562 and 594, indicating provenance from Pampean and Brasiliano belts (Pimentel et al., 1999, 2004, 2011; Rapela et al., 2007; Matteini et al., 2009) or Early Pampean/Late Brasiliano Arc (Hauser et al., 2010). Paleoproterozoic zircons, with a peak at 1955 Ma, and Arquean zircons, with a peak at 2621 Ma, indicates provenance from the Amazonian and/or Rio de la Plata Craton (Tassinari and Macambira, 1999; Rapela et al., 2007).

The younger main peak at 562 Ma, formed by seven zircons (Z11, 22, 50, 27, 55, 7 and 21), defines a concordia age of **569 ± 3 Ma**, which is interpreted in this paper as the maximum depositional age for the Chachapoyas Formation in the Mojotoro Range (Fig 5a). The minimum depositional age for this Formation is provided by the intrusion of felsic dikes at **533 Ma** (Aparicio González et al., 2011). Taking into account that the Chachapoyas Formation is strongly folded, the data indicates that the deposition and deformation of this supracrustal sequence took place in a short time interval, between 569 and 533 Ma. The range of sedimentation ages and geological constrains of the Chachapoyas Formation, it's suitable with the range ages of deposition and geological constraints of Puncoviscana Fm. *s.l* in the Tastil area (Fig. 1). Hauser et al. (2010) obtained a 562 Ma maximum depositional age for the Puncoviscana Formation *s.l* and a 534 ± 7 Ma minimum depositional age provided by the intrusion of a gray granodiorite. Therefore, the rock bearing the gray granodiorite in Tastil area is in a same stratigraphic unit as the Chachapoyas Formation.

The gray sandstone (CO 1) of the Alto de la Sierra Formation, shows a relative simple detrital zircon distribution with provenance ages between Late Neoproterozoic and Early Cambrian (~62% of the grains), suggesting a derivation from Pampean and Late Brasiliano/Early Pampean arcs (Hauser et al., 2010; Pimentel et al., 2011). The main peak, represented by the twelve younger zircons, defines a concordia age of **543 ± 1 Ma**. This age is interpreted as the maximum depositional age for the Alto de la Sierra Formation in the Mojotoro range.

The brown shaly sandstone (R 91) of Guachos Formation: shows a heterogeneous detrital zircon population with provenance

Table 2
Zircon U–Pb data for metasedimentary rocks of Alto de la Sierra Formation, Mojotoro range-NW Argentina.

Sample	Ratio						Rho	Ages						% Disc
	$^{207}Pb/^{206}Pb$	1σ (%)	$^{207}Pb/^{235}U$	1σ (%)	$^{206}Pb/^{238}U$	1σ (%)		$^{207}Pb/^{206}Pb$	1σ (Ma)	$^{207}Pb/^{235}U$	1σ (Ma)	$^{206}Pb/^{238}U$	1σ (Ma)	
Z3	0.05825	1.6	0.6852	2.0	0.08531	1.1	0.57	539.3	35.4	529.9	8.2	527.8	5.8	100
Z42	0.05827	1.2	0.6947	1.5	0.08647	0.8	0.55	539.9	26.8	535.6	6.2	534.6	4.2	100
Z48	0.05737	1.9	0.6872	2.2	0.08687	1.3	0.56	505.9	40.2	531.1	9.2	537.0	6.5	101
Z40	0.05843	0.8	0.7061	1.3	0.08764	1.1	0.78	545.9	18.1	542.4	5.6	541.6	5.5	100
Z47	0.05794	1.2	0.7002	1.8	0.08765	1.2	0.71	527.6	27.1	538.9	7.3	541.6	6.5	100
Z41	0.05834	1.3	0.7097	1.7	0.08824	1.0	0.62	542.5	28.3	544.6	7.0	545.1	5.4	100
Z9	0.05899	0.7	0.7196	1.3	0.08846	1.1	0.84	566.9	15.9	550.4	5.7	546.4	5.9	99
Z58	0.05818	1.5	0.7099	1.7	0.08850	0.7	0.43	536.6	33.3	544.7	7.2	546.7	3.8	100
Z10	0.05886	0.9	0.7186	1.2	0.08855	0.8	0.68	561.9	19.2	549.8	5.1	546.9	4.3	99
Z35	0.05844	2.3	0.7149	2.5	0.08872	0.9	0.37	546.5	50.1	547.7	10.6	548.0	4.9	100
Z21	0.05757	1.7	0.7061	2.5	0.08896	1.9	0.73	513.4	37.3	542.5	10.6	549.4	9.8	101
Z4	0.05830	1.3	0.7157	2.2	0.08904	1.8	0.82	540.9	28.0	548.1	9.4	549.9	9.6	100
Z24	0.05849	0.8	0.7249	1.4	0.08989	1.2	0.81	548.0	18.1	553.5	6.1	554.9	6.2	100
Z49	0.05798	1.0	0.7204	1.5	0.09012	1.1	0.72	528.9	22.1	550.9	6.2	556.2	5.7	101
Z31	0.05853	0.9	0.7276	1.2	0.09015	0.7	0.61	549.8	19.8	555.1	4.9	556.4	3.8	100
Z30	0.05845	1.0	0.7310	1.3	0.09070	0.8	0.64	546.6	21.1	557.1	5.4	559.7	4.3	100
Z29	0.05771	1.4	0.7247	1.7	0.09108	0.9	0.54	518.8	30.9	553.5	7.2	561.9	4.9	102
Z52	0.05815	0.8	0.7310	1.1	0.09117	0.7	0.68	535.6	16.9	557.2	4.5	562.5	3.9	101
Z33	0.05879	1.9	0.7448	3.0	0.09188	2.3	0.78	559.4	40.2	565.2	12.8	566.6	12.5	100
Z50	0.05869	2.5	0.7996	2.7	0.09882	1.0	0.37	555.5	53.3	596.6	12.0	607.5	5.8	102
Z34	0.06101	0.7	0.8727	1.3	0.10374	1.0	0.81	639.7	15.9	637.1	6.0	636.3	6.3	100
Z32	0.06007	1.3	0.8805	1.6	0.10632	0.9	0.58	606.0	27.4	641.3	7.4	651.3	5.6	102
Z13	0.06378	1.0	1.1601	1.6	0.13192	1.3	0.78	734.4	21.4	782.0	8.8	798.8	9.4	102
Z12	0.07444	0.9	1.9106	1.1	0.18614	0.7	0.59	1053.5	17.9	1084.8	7.4	1100.5	6.7	101
Z11	0.07559	1.0	1.9426	1.8	0.18638	1.6	0.84	1084.4	19.7	1095.9	12.3	1101.7	15.7	101
Z60	0.07658	0.8	2.0967	1.2	0.19857	0.9	0.78	1110.2	14.9	1147.7	8.2	1167.7	10.0	102
Z16	0.07920	5.2	1.9553	6.1	0.17906	3.3	0.53	1177.1	99.1	1100.3	40.3	1061.8	31.9	97
Z26	0.08487	0.6	2.7528	1.3	0.23525	1.1	0.88	1312.5	11.5	1342.8	9.5	1361.9	13.9	101
Z51	0.09498	0.8	3.3097	1.6	0.25274	1.4	0.88	1527.6	14.5	1483.3	12.7	1452.6	18.7	98
Z38	0.10532	0.7	4.7167	1.6	0.32482	1.4	0.89	1719.8	13.2	1770.2	13.1	1813.2	22.1	102
Z6	0.10747	0.9	5.1355	2.2	0.34659	2.0	0.91	1756.9	16.2	1842.0	18.3	1918.3	32.8	104
Z45	0.11734	2.7	5.4468	4.0	0.33667	2.9	0.73	1916.0	48.4	1892.3	33.7	1870.6	47.1	99
Z1	0.12447	3.0	6.9446	3.1	0.40464	0.8	0.28	2021.3	51.4	2104.4	26.9	2190.4	15.7	104
Z56	0.13485	0.6	7.3023	1.0	0.39274	0.7	0.77	2162.1	10.6	2149.1	8.6	2135.5	13.5	99
Z57	0.14998	0.6	9.2086	0.9	0.44530	0.7	0.75	2345.7	9.9	2359.0	8.0	2374.3	13.0	101
Z5	0.16199	0.7	11.0951	1.2	0.49675	0.9	0.79	2476.5	12.0	2531.1	10.9	2599.8	20.0	103
Z53	0.16371	0.7	11.0096	1.2	0.48774	0.9	0.79	2494.4	12.0	2523.9	10.7	2560.9	19.2	101

dominated by Neoproterozoic to Cambrian ages (~50% of the grains), indicating a main provenance from pre-tilcarian (Early Pampean/Late Brasiliano) (~560 Ma) and post-tilcarian (Pampean) sources (~530 Ma). The second important population, represented by the 35% of data, with peaks at 1004 and 1051 Ma, indicate provenance from the Sunsas–Grenvillian orogen (Cordani et al., 2000; Schwartz and Gromet, 2004).

The younger zircons, define a peak with a $^{206}Pb/^{238}U$ average age of **517 ± 5 Ma** (Fig. 4k). This age represent the maximum depositional age for the Guachos Formation in the Mojotoro range. Abundant zircons with morphology typical of felsic volcanic sources associated with a syn-sedimentary volcanism (Fig 5e,f) is a characteristic of this sequence. In terms of provenance and age, the Guachos Formation can be compared with the sediments of the Rancagua area. Lork et al. (1990) established an age between 560 and 530 Ma, whereas Adams et al. (2007, 2008) recognized a detrital zircon population in sandstones of the Rancagua area, indicating maximum sedimentation ages between 523 and 534 Ma. The zircons derived from felsic volcanic sources are registered in the rocks with fossil traces of *Nereites* Ichnofacies. The Guachos Formation is characterized by the *Nereites saltensis* (Aceñolaza y Alonso, 2000; Aparicio González et al., 2010; Seilacher et al., 2005). This ichnofacies have been associated with lower Cambrian traces by Seilacher et al. (2005) and Aparicio González et al. (2010), whereas López de Azarevich et al. (2012) recently related this with the late Ediacaran ages.

Therefore, the presence of acid volcanic material, tuffs or equivalents marks an event of great importance that can be taken as a guide level for recognizing clearly Cambrian units from the older ones (Aparicio González et al., 2010).

The sandstone L1, of Lizoite Formation, shows a simple zircon distribution age between 502 and 598 Ma. Inside this population, two main peaks, one at 555 Ma, and other at 533 Ma (inset Fig. 4h) are recognized. The four youngest zircons (Z56, 53, 52 and 32) define a concordia age of **513 ± 2 Ma,** which is interpreted as the maximum depositional age for Lizoite Formation in the Mojotoro range. The maximum depositional age for this unit, was also determined by others authors. Augustsson et al. (2011), obtained

Table 3
Zircon U–Pb data for metasedimentary rocks of Guachos Formation, Mojotoro range-NW Argentina.

Sample	Ratio						Rho	Ages						% Disc
	$^{207}Pb/^{206}Pb$	1σ (%)	$^{207}Pb/^{235}U$	1σ (%)	$^{206}Pb/^{238}U$	1σ (%)		$^{207}Pb/^{206}Pb$	1σ (Ma)	$^{207}Pb/^{235}U$	1σ (Ma)	$^{206}Pb/^{238}U$	1σ (Ma)	
Z50	0.05791	0.7	0.6313	2.3	0.07907	2.2	0.95	526.2	16.1	496.9	9.0	490.6	10.3	99
Z24	0.05880	0.6	0.6746	1.2	0.08321	1.0	0.85	559.6	13.8	523.5	4.9	515.2	5.1	98
Z32	0.05784	0.9	0.6666	1.3	0.08359	1.0	0.73	523.7	19.7	518.7	5.4	517.5	4.8	100
Z25	0.05903	0.8	0.6806	1.1	0.08362	0.8	0.67	568.3	18.3	527.1	4.7	517.7	3.8	98
Z26	0.05879	0.9	0.6792	1.5	0.08379	1.2	0.81	559.4	18.6	526.3	6.0	518.7	5.9	99
Z3	0.05794	0.7	0.6843	1.1	0.08565	0.9	0.81	527.5	14.4	529.3	4.7	529.8	4.7	100
Z18	0.05774	0.7	0.6920	1.0	0.08693	0.7	0.70	519.9	16.1	534.0	4.3	537.3	3.7	101
Z44	0.05821	0.8	0.7088	1.7	0.08831	1.5	0.88	537.8	17.1	544.1	7.0	545.6	7.7	100
Z34	0.05917	1.5	0.7218	1.9	0.08848	1.1	0.59	573.5	32.4	551.8	7.9	546.5	5.8	99
Z46	0.05828	1.0	0.7163	1.3	0.08915	0.8	0.66	540.2	20.8	548.5	5.4	550.5	4.4	100
Z14	0.05876	0.6	0.7300	1.0	0.09011	0.8	0.78	558.1	13.6	556.6	4.3	556.2	4.2	100
Z51	0.05871	0.7	0.7299	1.6	0.09016	1.5	0.91	556.4	14.5	556.5	6.8	556.5	7.8	100
Z15	0.05744	1.1	0.7166	1.5	0.09049	1.0	0.67	508.5	24.9	548.7	6.5	558.4	5.4	102
Z8	0.05813	1.7	0.7437	1.4	0.09279	0.8	0.59	534.8	35.9	564.6	6.2	572.0	4.6	101
Z12	0.05809	2.0	0.7670	1.5	0.09577	1.3	0.82	533.0	42.8	578.0	6.7	589.6	7.1	102
Z36	0.05822	0.6	0.7763	1.7	0.09671	1.5	0.93	538.0	13.2	583.4	7.3	595.1	8.7	102
Z04	0.05865	0.9	0.7840	3.3	0.09696	3.2	0.96	554.0	19.1	587.8	14.7	596.6	18.2	101
Z5	0.06114	0.5	0.8894	1.2	0.10551	1.1	0.90	644.0	11.6	646.0	5.8	646.6	6.8	100
Z27	0.06193	0.6	0.9069	0.8	0.10621	0.5	0.66	671.8	12.8	655.4	3.8	650.7	3.3	99
Z7	0.06068	1.0	0.9215	0.8	0.11015	0.6	0.79	627.7	20.7	663.1	3.7	673.6	3.8	102
Z6	0.06213	0.5	1.0335	1.0	0.12065	0.9	0.89	678.4	9.9	720.7	5.3	734.3	6.4	102
Z60	0.06546	1.4	1.1730	3.1	0.12995	2.8	0.90	789.3	28.7	788.0	17.0	787.6	20.8	100
Z45	0.06566	0.8	1.2129	1.6	0.13397	1.4	0.87	795.7	15.9	806.5	8.6	810.5	10.3	100
Z48	0.06994	0.5	1.5136	1.0	0.15697	0.8	0.85	926.5	10.5	935.9	5.8	939.9	7.1	100
Z10	0.07116	2.9	1.6475	4.6	0.16791	3.6	0.78	962.1	57.5	988.6	28.7	1000.6	33.2	101
Z11	0.07116	0.6	1.7087	0.9	0.17415	0.7	0.76	962.1	11.5	1011.8	5.5	1034.9	6.3	102
Z52	0.07166	0.7	1.6142	1.5	0.16338	1.3	0.87	976.2	14.7	975.8	9.2	975.5	11.6	100
Z21	0.07174	0.5	1.6822	1.0	0.17005	0.9	0.85	978.7	11.1	1001.8	6.6	1012.4	8.3	101
Z33	0.07252	0.5	1.7509	1.1	0.17512	0.9	0.88	1000.4	10.0	1027.5	6.8	1040.3	8.9	101
Z43	0.07253	0.6	1.7384	1.5	0.17385	1.4	0.93	1000.7	11.3	1022.9	9.8	1033.3	13.6	101
Z22	0.07254	0.6	1.7442	0.9	0.17439	0.7	0.77	1001.1	11.6	1025.0	5.8	1036.3	6.6	101
Z30	0.07297	0.9	1.8837	2.5	0.18723	2.4	0.94	1013.1	17.8	1075.4	16.7	1106.3	24.1	103
Z17	0.07318	0.5	1.8581	1.6	0.18416	1.5	0.94	1018.9	10.6	1066.3	10.4	1089.7	14.9	102
Z58	0.07396	0.6	1.9058	2.6	0.18689	2.5	0.98	1040.3	11.4	1083.1	17.2	1104.5	25.7	102
Z57	0.07413	0.9	1.9059	2.6	0.18647	2.4	0.94	1045.0	17.5	1083.1	16.8	1102.2	24.2	102
Z37	0.07420	0.6	1.9787	1.2	0.19341	1.1	0.88	1046.9	11.4	1108.3	8.0	1139.8	11.0	103
Z9	0.07460	0.6	1.8353	0.9	0.17844	0.7	0.79	1057.6	11.0	1058.2	5.9	1058.4	6.9	100
Z30	0.07530	1.1	1.8674	2.7	0.17985	2.5	0.92	1076.6	21.3	1069.6	17.6	1066.2	24.1	100
Z1	0.08359	0.6	2.5183	1.0	0.21850	0.8	0.81	1283.0	11.5	1277.3	7.3	1274.0	9.4	100
Z31	0.11222	0.7	5.4356	1.9	0.35130	1.8	0.93	1835.7	12.3	1890.5	16.0	1940.8	29.3	103
Z2	0.11441	0.5	5.2131	0.9	0.33048	0.7	0.83	1870.6	8.9	1854.8	7.4	1840.7	11.5	99
Z31	0.11469	0.8	5.6311	2.1	0.35609	2.0	0.93	1875.0	14.2	1920.9	18.3	1963.6	33.6	102
Z23	0.11515	0.5	5.2471	1.0	0.33048	0.9	0.87	1882.3	9.0	1860.3	8.6	1840.7	14.0	99
Z59	0.12579	0.8	6.2216	2.2	0.35873	2.0	0.94	2039.9	13.5	2007.5	18.9	1976.1	34.6	98
Z40	0.17821	2.2	12.1618	4.1	0.49496	3.5	0.85	2636.3	35.9	2617.0	37.7	2592.1	73.5	99
Z35	0.18277	0.8	12.3674	1.1	0.49076	0.8	0.71	2678.2	12.4	2632.7	10.0	2574.0	16.2	98

and age of 517 ± 4 Ma for Lizoite Fm. in Angosto, Perchel and Huacalera locality (Humahuaca Valley), whereas Adams (2011) determined in the Mojotoro Range a small volcanic zircon (Fig 5g,h) age group, c. 500 Ma (Late Cambrian). These ages are absent in the Puncoviscana Complex and thus sets it's a younger depositional age limit.

Finally, our data indicates that the sedimentation of the Puncoviscana Complex continued after 533–534 Ma, like the U–Pb results of the Guachos Formation detritic zircons shows. Therefore, the sedimentation and deformation of the Chachapoyas Formation took places between 569 Ma to 533 Ma.

The data indicate the presence of **two tecto-magmatic events**. The **first tecto-magmatic event** is associated with the deformation and metamorphism of the Chachapoyas Formation and equivalent units, named here as Tilcara I.

After this stage, the rocks were intruded by a first magmatic pulse of lower Cambrian age (for example, the gray granodiorite facies of Tastil batholith and Mojotoro intrusive). The tuff identified in Santa Victoria locality (Fig. 1) (Escayola et al., 2011) correlate whit this magmatic event. The detailed geologic mapping of the Chachapoyas Formation allowed to observe that there is a fault contact with the Guachos Formation; this fault can be a previous discontinuity of the classic Tilcara discordance (Aparicio González et al., 2010) (Tilcara Unconformity I) (Fig. 6).

Subsequently, the sedimentation of the Alto de la Sierra and Guachos Formations and the equivalent units identified in the area of Rancagua, Ampujaco (Tucumán), El Carmen (Salta-Jujuy) and Quebrada La Rioja (La Rioja) occurred. Their maximum sedimentation ages are 543 Ma and lower values (Adams et al., 2008, 2011). These units are affected by a **second tecto-magmatic event**, the Tilcara II, whose main evidences include the late lower Cambrian intrusive, as the Chañi granite (511 Ma). The Guachos Formation is separated from the Lizoite Formation (Mesón Group) by a classic angular discordance defined by Turner (1960) (Fig. 6).

Table 4
Zircon U–Pb data for metasedimentary rocks of Lizoite Formation, Mojotoro range-NW Argentina.

Sample	Ratio						Rho	Ages						% Disc
	$^{207}Pb/^{206}Pb$	1σ (%)	$^{207}Pb/^{235}U$	1σ (%)	$^{206}Pb/^{238}U$	1σ (%)		$^{207}Pb/^{206}Pb$	1σ (Ma)	$^{207}Pb/^{235}U$	1σ (Ma)	$^{206}Pb/^{238}U$	1σ (Ma)	
Z6	0.05862	0.8	0.6554	2.2	0.08110	2.1	0.93	552.9	18.1	511.8	8.9	502.7	9.9	98
Z56	0.05784	1.2	0.6536	1.6	0.08196	1.1	0.68	523.7	25.2	510.7	6.3	507.8	5.3	99
Z53	0.05758	0.7	0.6586	1.0	0.08296	0.8	0.73	513.7	15.5	513.8	4.2	513.8	3.7	100
Z52	0.05768	1.5	0.6606	2.1	0.08305	1.4	0.67	517.8	33.5	515.0	8.4	514.3	7.0	100
Z32	0.05761	1.3	0.6607	1.5	0.08318	0.8	0.52	514.9	27.3	515.0	5.9	515.1	3.8	100
Z55	0.05751	0.6	0.6694	0.9	0.08442	0.6	0.68	511.3	13.8	520.4	3.5	522.4	2.9	100
Z10	0.05815	1.4	0.6773	1.5	0.08448	0.7	0.43	535.5	29.8	525.2	6.2	522.8	3.3	100
Z27	0.05750	1.0	0.6707	1.5	0.08460	1.1	0.74	510.6	22.2	521.1	6.2	523.5	5.6	100
Z58	0.05837	0.6	0.6825	1.3	0.08480	1.2	0.90	543.7	12.8	528.3	5.5	524.7	6.0	99
Z20	0.05832	0.9	0.6826	1.2	0.08489	0.9	0.69	541.7	19.4	528.4	5.1	525.3	4.3	99
Z57	0.05791	1.0	0.6782	1.8	0.08494	1.5	0.83	526.2	21.5	525.7	7.3	525.6	7.5	100
Z36	0.05803	0.7	0.6806	1.0	0.08506	0.8	0.78	530.7	14.2	527.1	4.2	526.3	4.1	100
Z21	0.05832	1.6	0.6845	2.0	0.08513	1.2	0.61	541.7	33.9	529.5	8.1	526.7	6.1	99
Z5	0.05789	1.0	0.6799	2.7	0.08518	2.5	0.93	525.5	22.1	526.7	11.2	527.0	12.9	100
Z54	0.05786	0.8	0.6822	1.2	0.08550	0.9	0.75	524.6	17.0	528.1	4.9	528.9	4.5	100
Z23	0.05837	0.8	0.6898	1.2	0.08571	0.9	0.76	543.7	16.8	532.7	4.9	530.1	4.5	100
Z26	0.05791	1.5	0.6874	2.0	0.08610	1.3	0.64	526.3	33.6	531.3	8.3	532.4	6.6	100
Z9	0.05763	0.9	0.6848	1.1	0.08617	0.7	0.61	515.9	19.7	529.6	4.7	532.8	3.5	101
Z22	0.05887	0.9	0.7000	1.3	0.08625	1.0	0.72	562.1	19.7	538.8	5.5	533.3	4.9	99
Z29	0.05758	1.7	0.6856	2.0	0.08636	1.0	0.48	513.6	37.9	530.2	8.2	534.0	4.9	101
Z25	0.05794	1.4	0.6904	1.7	0.08642	0.8	0.51	527.4	30.8	533.0	6.8	534.3	4.3	100
Z42	0.05913	0.8	0.7052	1.2	0.08650	0.8	0.70	571.8	18.2	541.9	4.9	534.8	4.2	99
Z41	0.05839	0.8	0.6988	1.2	0.08680	0.9	0.74	544.4	17.3	538.1	4.9	536.6	4.5	100
Z46	0.05847	0.6	0.7063	1.4	0.08761	1.3	0.90	547.4	13.7	542.5	6.1	541.4	6.8	100
Z4	0.05825	1.0	0.7058	1.5	0.08788	1.0	0.72	539.3	22.0	542.3	6.1	543.0	5.4	100
Z18	0.05809	1.3	0.7051	1.7	0.08803	1.1	0.64	533.2	29.0	541.8	7.3	543.9	5.9	100
Z45	0.05878	0.8	0.7169	2.1	0.08846	2.0	0.93	559.0	16.5	548.9	8.9	546.4	10.3	100
Z2	0.05832	1.0	0.7122	1.6	0.08858	1.2	0.79	541.7	21.0	546.1	6.6	547.1	6.4	100
Z51	0.05807	1.3	0.7105	1.7	0.08875	1.1	0.67	532.3	27.8	545.1	7.2	548.1	6.0	101
Z28	0.05754	0.8	0.7048	1.2	0.08884	0.9	0.75	512.3	17.6	541.7	5.1	548.7	4.8	101
Z14	0.05913	1.9	0.7261	2.0	0.08906	0.7	0.33	571.7	41.3	554.3	8.7	550.0	3.5	99
Z16	0.05875	1.3	0.7271	1.7	0.08977	1.0	0.61	557.7	28.5	554.8	7.1	554.2	5.4	100
Z35	0.05782	0.6	0.7164	1.4	0.08987	1.3	0.89	522.8	13.7	548.5	5.9	554.8	6.6	101
Z15	0.05928	1.8	0.7348	3.8	0.08989	3.3	0.88	577.4	38.0	559.3	16.1	554.9	17.7	99
Z19	0.05834	0.9	0.7242	1.2	0.09003	0.7	0.62	542.6	20.2	553.1	5.1	555.7	3.9	100
Z11	0.05833	0.8	0.7244	1.1	0.09007	0.8	0.73	542.1	16.9	553.2	4.9	555.9	4.5	100
Z17	0.05859	1.6	0.7289	1.7	0.09023	0.6	0.37	551.9	34.5	555.9	7.3	556.9	3.4	100
Z13	0.05825	0.6	0.7266	0.9	0.09047	0.7	0.74	539.0	13.8	554.5	4.0	558.3	3.7	101
Z59	0.05829	0.7	0.7366	1.5	0.09165	1.3	0.89	540.5	15.0	560.4	6.5	565.3	7.3	101
Z1	0.05831	0.8	0.7376	1.5	0.09176	1.2	0.84	541.3	17.2	561.0	6.3	565.9	6.8	101
Z12	0.05798	0.7	0.7339	0.9	0.09181	0.7	0.71	528.8	14.3	558.8	4.0	566.2	3.6	101
Z33	0.05885	1.2	0.7893	1.6	0.09727	0.9	0.61	561.7	26.8	590.8	7.0	598.4	5.4	101
Z31	0.06927	0.7	1.3345	1.2	0.13973	1.0	0.80	906.8	15.1	860.9	7.0	843.1	7.6	98
Z8	0.07332	0.6	1.6931	0.9	0.16747	0.7	0.75	1022.9	12.4	1005.9	5.9	998.2	6.4	99
Z44	0.07425	0.9	1.8765	1.2	0.18330	0.8	0.69	1048.2	17.7	1072.8	8.0	1085.0	8.4	101
Z7	0.07451	0.7	1.7827	1.0	0.17353	0.7	0.68	1055.3	14.8	1039.2	6.6	1031.5	6.6	99
Z50	0.11415	0.5	5.3107	1.5	0.33743	1.4	0.94	1866.5	9.3	1870.6	13.0	1874.3	23.5	100
Z49	0.12089	0.5	6.0420	1.9	0.36249	1.9	0.97	1969.4	8.4	1981.9	16.8	1994.0	32.2	101
Z24	0.19361	0.5	14.9218	1.0	0.55898	0.9	0.85	2773.1	8.9	2810.3	9.8	2862.4	20.3	102

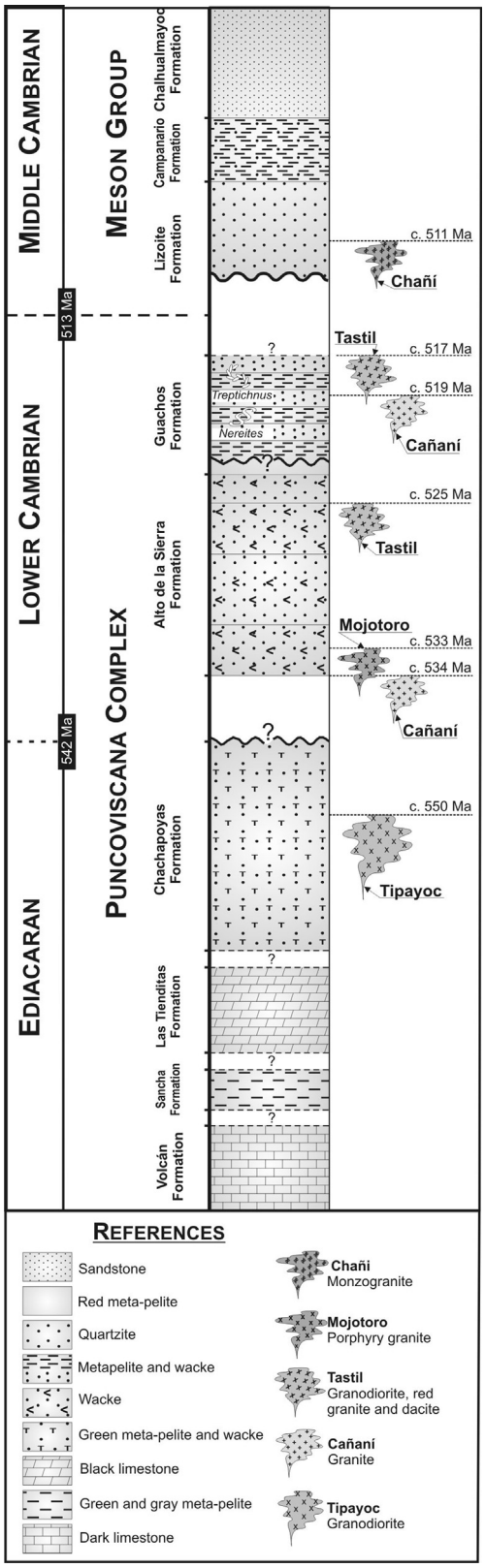

Fig. 6. Stratigraphic column showing the stratigraphic relationship of the different units defined in the Eastern Cordillera and the ages of the main intrusive rocks. Esta figura me parece que hay que mejorarla.

We consider that the Puncoviscana Complex in the Mojotoro Range is a significative stratigraphic model to be applied in other areas of the Eastern Cordillera.

We demonstrated that heterogeneous ages U–Pb of the detrital zircon in Puncoviscana Complex indicated different times of sedimentation for the stratigraphic units studied in this paper.

Acknowledgments

The first author thanks CONICET for the scholarship granted. Thanks Laura and Muriel for revising the English text. I appreciate the help of N. Uriz for making some of the figures. I would also like to thank the valuable recommendations made by Dr. Maximiliano Naipauer which helped improve the manuscript. The reviewer and anonymous reviewer are gratefully acknowledged

References

Adams, C.J., Miller, H., Toselli, A.J., 2007. Detrital zircon ages of the Puncoviscana Formation of NW Argentina, and their bearing on stratigraphic age and provenance. In: 20th Colloquium on Latin American Earth Sciences Kiel, pp. 68–69. Germany. Abstracts.

Adams, C.J., Miller, H., Toselli, A.J., Griffin, W.L., 2008. The Puncoviscana formation of northwest Argentina: U–Pb geochronology of detrital zircons and Rb–Sr metamorphic ages and their bearing on its stratigraphic age, sediment provenance and tectonic setting. Neues Jahrb. Geol. Palaöntol. Abhand. 247, 341–352.

Adams, C.J., 2011. The Pacific Gondwana margin in the late Neoproterozoic–early Paleozoic: detrital zircon U–Pb ages from metasediments in northwest Argentina reveal their maximum age, provenance and tectonic setting. Gondwana Res. 19, 71–83.

Aceñolaza, F.G., Toselli, A.J., 1973. Consideraciones estratigráficas y tectónicas sobre el Paleozoico inferior del Noroeste Argentino. In: Memorial del II Congreso Latinoamericano de Geología, Caracás, vol. 2. Ministerio de Minas e Hidrocarburos, Dirección de Geología, Caracas, pp. 755–764.

Aceñolaza, F.G., Miller, H., Toselli, A.J., 1988. The Puncoviscana Formación (Late Precambrian-Early Cambrian). Sedimentology, tectonometamorphic history and age of the oldest rocks of NW Argentina. In: Bahlburg, H., Breitkreuz, Ch., Giese, P. (Eds.), The Southern Central Andes, Lecture Notes in Earth Sciences, vol. 17, pp. 25–37.

Aceñolaza, F.G., Miller, H., Toselli, A.J. (Eds.), 1990. El Ciclo Pampeano en el Noroeste Argentino. Serie de Correlacion Geológica. Universidad Nacional de Tucumán, pp. 1–227.

Aceñolaza, F.G., Alonso, R., 2000. La formación Puncoviscana *s.l.* a partir de nuevos elementos icnológicos en la provincia de Salta. Rev. Asoc. Geol. Argent. Ameghiniana 37, 4.

Aceñolaza, F.G., Aceñolaza, G., 2005. La Formación Puncoviscana y unidades estratigráficas vinculadas en el Neoproterozoico-Cámbrico Temprano del Noroeste Argentino. Latin Am. J. Sedimentol. Basin Anal. 12, 65–87.

Amengual, R., Mendez, V., Navarini, A., Viera, O., Zanettini, J.C., 1979. Geología de la región noroeste argentino. In: Segundo Congreso Latinoamericano de Geología. Caracas 2, pp. 755–763.

Aparicio González, P.A., Moya, M.C., Impiccini, A., 2010. Estratigrafía del basamento Neoproterozoico – Cámbrico, Sierra de Mojotoro, Cordillera Oriental Argentina. Latin Am. J. Sedimentol. Basin Anal. 17, 65–83.

Aparicio González, P.A., Pimentel, M., Hauser, N., 2011. Datación U –Pb por LA ICPMS de diques graníticos del ciclo Pampeano, sierra de Mojotoro, Cordillera Oriental argentina. Rev. Asoc. Geol. Argent. 68, 33–38.

Augustsson, C., Rüsing, T., Adams, C.J., Chmiel, H., Kocabayoglu, M., Büld, M., Zimmermann, U., Berndt, J., Kooijman, E., 2011. Detrital quartz and zircon combined: the production of mature sand with short transportation paths along the Cambrian west Gondwana margin, northwestern Argentina. J. Sediment. Res. 81, 284–298.

Bachmann, G., Grauert, B., Kramm, U., Lork, A., Miller, H., 1987. El magmatismo del Cambrico medio/Cambrico Superior en el basamento del noroeste Argentina; investigaciones isotópicas y geocronológicas sobre los granitoides de los complejos intrusivos de Santa Rosa de Tastil y Cañani. Actas Cong. Geol. Argent. 4, 125–127.

Baldis, B.A., Omarini, R., 1984. El Grupo Lerma (Precámbrico-Cámbrico) en la comarca central salteña y su posición en el borde pacífico americano. In: Acta 9° Congreso Geológico Argentino. S. C. Bariloche, vol. 1, pp. 64–78.

Cawood, P.A., 2005. Terra australis Orogen: Rodinia breakup and development of the Pacific and Iapetus margins of Gondwana during the Neoproterozoic and Paleozoic. Earth Sci. Rev. 69, 249–279.

Cordani, U.G., Sato, K., Teixeira, W., Tassinari, C.C.G., Basei, M.A.S., 2000. Crustal evolution of the South American Platform. In: Cordani, U.G., Milani, E.J., Thomaz Filho, A., Campos, D.A. (Eds.), Tectonic Evolution of South America. 31st International Geological Congress. Río de Janeiro, Brazil, pp. 19–40.

Cordani, U.G., Brito-Neves, B.B., D'Agrella, M.S., 2003. From Rodinia of Gondwana: a review of the available evidence from South America. Gondwana Res. 6, 275–283.
Do Campo, M., Guevara, S Ribeiro, 2005. Provenance análisis and tectonic setting of Late Neoproterozoic metasedimentary successions in NW Argentina. J. S. Am. Earth Sci. 19, 143–145.
Escayola, M.P., Van Staal, C.R., Davis, W.J., 2011. The age and tectonic setting of the Puncoviscana Formation in northwestern Argentina: an accretionary complex related to Early Cambrian closure of the Puncoviscana Ocean and accretion of the Arequipa-Antofalla block. J. S. Am. Earth Sci. 32, 438–459.
Hallsworth, C.R., Knox, R.W.O.'B., 1999. BGS Rock Classification Scheme. In: Classification of Sediments and Sedimentary Rocks, vol. 3. British Geological Survey, pp. 1–44. Research Report, RR 99-03.
Harrington, H.J., Leanza, A.F., 1957. Ordovician Trilobites of Argentina, vol. 1. Department of Geology, University of Kansas, p. 276. Special Publication.
Hauser, N., Matteini, M., Omarini, R.H., Pimentel, M.M., 2010. Combined U–Pb and Lu–Hf isotope data on turbidites of the Paleozoic basement of NW Argentina and petrology of associated igneous rocks: Implications for the tectonic evolution of western Gondwana between 560 and 460 Ma. Gondwana Res. 19 (1), 100–127.
Hongn, F.D., 1996. La Estructura Pre-Grupo Mesón (Cámbrico) del Basamento del Valle de Lerma, Provincia de Salta. Acta 13° Cong. Geol. Argent., 137–145.
Hongn, F.D., Tubia, J.M., Aranguren, A., Vegas, N., Mon, R., Dunning, G., 2010. Magmatism coeval with lower Paleozoic shelf basins in NW-Argentina (Tastil batholith): constraints on current stratigraphic and tectonic interpretations. J. S. Am. Earth Sci. 29, 289–305.
Jackson, S.E., Pearson, N.J., Griffin, W.L., Belousava, E.A., 2004. The application of laser ablation–inductively coupled plasma-mass spectrometry (LA–ICP-MS) to in situ U–Pb zircon geochronology. Chem. Geol. 211, 47–69.
Jezek, P., 1990. Análisis Sedimentológico de la Formación Puncoviscana entre Tucumán y Salta. In: Aceñolaza, F.G., Miller, H., Toselli, A.J. (Eds.), El Ciclo Pampeano en el Noreste Argentino, Serie Correlación Geológica, vol. 4. (UNT. Facultad de Ciencias Naturales e Instituto Miguel Lillo. Instituto Superior de Correlación Geológica), Tucumán, pp. 9–36.
Keidel, J., 1910. Estudio geológico en la quebrada de Humahuaca y en la de Iruya. Anal. Minist. Agricult. Secc. Geol. Mineral. Minería 5, 76–77.
Keidel, J., 1943. El ordovícico inferior en los Andes del Norte argentino y sus depósitos marinos-glaciales. Acad. Nacion. Cienc. Córdoba, Bol. 36, 140–229.
Keppie, J.D., Bahlburg, H., 1999. Puncoviscana Formation of northwestern and central Argentina. In: Ramos, V.A., Keppie, J.D. (Eds.), Laurentia-Gondwana Connections before Pangea. Geological Society of America, pp. 139–143. Special Paper 336.
Kraemer, P., Escayola, M., Martino, R., 1995. Hipótesis sobre la evolución tectónica neoproterozoica de las Sierras Pampeanas de Córdoba (30° 40′ – 32° 40′S) Argentina. Rev. Asoc. Geol. Argent. 50, 47–50.
López de Azarevich, V., Aceñolaza, F.G., Omarini, R., Azarevich, M., 2012. La Cuenca Neoproterozoica – Eocámbrica en el NOA: sedimentología y ambientes de depósito de secuencias con icnofósiles, nuevas perspectivas. In: XIII Reunión Argentina de Sedimentología, Relatorio, pp. 119–132.
Lork, A., Miller, H., Kramm, U., Grauert, B., 1990. Sistemática U–Pb de circones detríticos de la Fm. Puncoviscana y su significado para la edad máxima de sedimentación en la Sierra de Cachi (prov. de Salta, Argentina). In: Aceñolaza, F.G., Miller, H., Toselli, A.J. (Eds.), El Ciclo Pampeano en el Noroeste Argentino, Serie de Correlación Geológica N 4. Universidad de Tucumán, pp. 199–208.
Lucassen, F., Becchio, R., Wilke, H., Franz, G., Thirwall, M., Viramonte, J.G., Wemmer, K., 2000. Proterozoic-Paleozoic development of the basement of the Central Andes (18–26°) a mobile belt of the South America craton. J. S. Am. Earth Sci. 13, 697–715.
Ludwig, K.R., 2003. Special Publication. User's Manual for Isoplot/Ex rev.3.00: a Geochronological Toolkit for Microsft Excel, vol. 4. Berkeley Geochronology Center, Berkeley, California, U.S.A.
Llambías, E.J., Sato, A.M., Ortíz Suarez, A., Proxy, C., 1998. The granitoids of the Sierra de San Luis. In: Pankhurst, R.J., Rapela, C.W. (Eds.), The Proto-Andean Margin of Gondwana, vol. 142. Geological Society of London, pp. 325–341. Special Publications.
Mángano, M.G., Buatois, L.A., 2004. Integración de estratigrafía secuencial, sedimentología e icnología para un análisis cronoestratigráfico del Paleozoico inferior del noroeste argentino. Rev. Asoc. Geol. Argent. 59, 273–280.
Matteini, M., Junges, S.L., Dantas, E.L., Pimentel, M.M., Bühn, B., 2009. In situ zircon U-Pb and Lu–Hf isotope systematic on magmatic rocks: insights on the crustal evolution of the Neoproterozoic Goiás Magmatic Arc, Brasília belt, Central Brazil. Gondwana Res. 16, 200–212.
Meert, J.G., Torsvik, T.H., 2003. The making unmaking of a supercontinent: Rodinia revisited. Tectonophysics 375, 261–288.
Mirré, J.C., Aceñolaza, F.G., 1972. El hallazgo de Oldhamia isp. (traza fósil) y su valor como evidencia de edad cámbrica para el supuesto Precámbrico del borde occidental del Aconquija, Provincia de Catamarca. Ameghiniana 9, 72–78.
Moya, M.C., 1998. El Paleozoico inferior en la sierra de Mojotoro, Salta–Jujuy. Rev. Asoc. Geol. Argent. 53, 219–238.
Moya, M.C., 2008. El Paleozoico inferior en el noroeste argentino. Evidencias, incógnitas, propuestas para la discusión. In: Coira, B., Zappettini, E. (Eds.), Geología y Recursos Naturales de la Provincia de Jujuy, Relatorio del XVII Congreso Geológico Argentino, S.S. de Jujuy, pp. 74–84.
Omarini, R.H., Sureda, R.J., Gotze, H.J., Seilacher, A.Y., Pfluger, F., 1999. Puncoviscana folded belt in northwestern Argentina: testimony of Late Proterozoic Rodinia fragmentation and pre-Gondwana collisional episodes. Int. J. Earth Sci. 88, 76–97.
Pimentel, M.M., Fuck, R.A., Botelho, N.F., 1999. Granites and the geodynamic history of the Neoproterozoic Brasilia belt, Central Brazil: a review. Lithos 46, 463–483.
Pimentel, M.M., Ferreira Filho, C.F., Armstrong, R.A., 2004. SHRIMP U-Pb and Sm-Nd ages of the Niquelândia layered complex: Meso-(1.25 Ga) and Neoproterozoic (0.79 Ga) extensional events in central Brazil. Precambrian Res. 132, 133–153.
Pimentel, M.M., Rodrigues, J.B., Della Giustina, M.E.S., Junges, S.L., Matteini, M., 2011. The tectonic evolution of the Brasilia Belt, central Brazil, based on SHRIMP and LA-ICPMS U-Pb sedimentary provenance data. J. S. Am. Early Sci. 31, 345–357.
Ramos, V.A., 1988. Tectonics of the Late Proterozoic-Early Paleozoic: a collisional history of southern South America. Episodes 11, 168–174. Ottawa.
Ramos, V.A., 2008. The basement of the central Andes: the Arequipa and related Terranes. Annu. Rev. Earth Planet. Sci. 36, 289–324.
Rapela, C.W., Casquet, C., Baldo, E., Dahlquist, J., Pankhurst, R.J., Galindo, C., Saavedra, J., 2001. Las Orogénesis del Paleozoico Inferior en el margen proto-andino de América del Sur Sierras pampeanas, Argentina. J. Iber. Geol. 27, 23–41.
Rapela, C.W., Pankhurst, R.J., Casquet, C., Fanning, C.M., Baldo, E.G., González-Casado, J.M., Galindo, C., Dahlquist, J., 2007. The Río de la Plata craton and the assembly of SW Gondwana. Earth Sci. Rev. 83, 49–82.
Salfity, J.A., Omarini, R.H., Baldis, B., Gutiérrez, W., 1975. Consideraciones sobre la evolución geotectónica del Precámbrico y Paleozoico Inferior del Norte de Argentina. In: Acta 2° Congreso Iberoamericano de Geología Económica, vol. 4, pp. 341–361.
Schwartz, J.J., Gromet, L.P., 2004. Provenance of a late Proterozoic-early Cambrian basin, Sierras de Córdoba, Argentina. Precambrian Res. 129, 1–21.
Schwartz, J., Gromet, L., Miro, R., 2008. Timing and duration of the Calc-Alkaline Arc of the Pampean Orogeny implications for the Late neoproterozoic to Cambrian evolution of Western Gondwana. J. Geol. 116, 39–61.
Seilacher, A., Buatois, L.A., Mángano, M.G., 2005. Trace fossils in the Ediacaran-Cambrian transition: behavioral diversification, ecological turnover and environmental shift. Palaeogeogr. Palaeoclimatol. Palaeoecol. 227, 323–356.
Sims, P., Ireland, T.R., Camacho, A., Lyons, P., Pieters, P.E., Skirrow, R.G., Stuart-Smith, P.G., Miró, R., 1998. U–Pb, Th–Pb and Ar–Ar geochronology from the southern Sierras pampeanas, Argentina: implications for the Palaeozoic tectonic evolution of the western Gondwana margin. In: Pankhurst, R.J., Rapela, C.W. (Eds.), The Proto-Andean Margin of Gondwana, vol. 142. Geological Society, London, pp. 259–281. Special Publications.
Stacey, J.S., Kramers, J.D., 1975. Approximation of terrestrial lead isotope evolution by a two stage model. Earth Planet. Sci. Lett. 26, 207–221.
Tassinari, C.C.G., Macambira, M.J.B., 1999. Geochronological provinces of the Amazonian Craton. Episodes 22, 174–182.
Turner, J.C.M., 1960. Estratigrafía de la Sierra de Santa Victoria y adyacencias. Bolet. Acad. Nacion. Cienc. Córdoba 41, 163–196.
Vaughan, A.P.M., Pankhurst, R.J., 2008. Tectonic overview of the West Gondwana margin. Gondwana Res. 13, 150–162.
Willner, A.P., 1990. División tectometamórfica del Basamento del Noroeste Argentino. In: Aceñolaza, F., Miller, H., Toselli, A.J. (Eds.), El Ciclo Pampeano en el Noroeste Argentino, Serie de Correlación Geológica, vol. 4, pp. 113–159.
Zappettini, E.O., Coira, B., Santos, J.O., 2008. Edad U/Pb de la Formación Chañi: un granito del arco magmático Tilcárico. In: Xvii Congreso Geológico Argentino, Jujuy, vol. 2, pp. 248–249.
Zimmermann, U., 2005. Provenance studies of very low to low-grade metasedimentary rocks of the Puncoviscana Complex, northwest Argentina. In: Vaughan, A.P.M., Leat, P.T., Pankhurst, R.J. (Eds.), Terrane Processes at the Margins of Gondwana, vol. 246. Geological Society, London, pp. 381–416. Special Publications.